VIBRATION CONTROL ON ACTIVE MAGNETIC BEARING EQUIPPED FLYWHEEL ROTOR

Keiji Katsuno, Graduate student
Department of Mechanical Engineering, The National Defense Academy
Hasirimizu, Yokosuka, Kanagawa, Japan

Hiroki Okubo, Lecturer, Dr.
Department of Mechanical Engineering, The National Defense Academy

Hiroyuki Fujiwara, Research Associate, Dr.
Department of Mechanical Engineering, The National Defense Academy

Osami Matsushita, Professor, Dr.
Department of Mechanical Engineering, The National Defense Academy

ABSTRACT

Flywheel technology has been developing for an effective and clean means of energy storage techniques. From the point of view of the improvement for the stable rotation during high speed revolution, we employed the active magnetic bearing (AMB) to apply it to a flywheel test rotor. Our AMB equipped flywheel rotor is levitated without mechanical contact by five-axis controllers in the decentralized manner: three positions to vertically suspend this flat rotor and two X and Y rotations to maintain the rotor at a neutral position.

In this paper, we propose several ideas in numerical simulations concerning the AMB control method for the stability improvement of this flywheel rotor. An equivalent reduced model of the rotor is first completed from the quasi-modal method. The traditional PID control is mainly applied to the standstill levitation. This PID controller is not able to cover the stability in the entire speed range, because natural frequencies split into two ways due to the strong gyroscopic effect: the increase of the forward eigenfrequency and the decrease of the backward eigenfrequency. In order to compensate the destabilization caused by this split, we recommend the addition of an optional technique of the cross stiffness control. The simulation proves that the cross stiffness control should be combined with a band-pass filter for selecting the forward eigenmode vibration and a low pass filter for tuning the backward mode vibration. We also consider the spillover instability due to the flexibility of the flywheel disk.

1 INTRODUCTION

Flywheel has been used for a long time. It has attracted the attention as an energy storage system[1],[2],[3]. Large flywheel with low rotation has already put into practical use in several instances. The small flywheel with high speed rotation used for more than eight hours has been developing. Several dynamic problems still remain, e.g., energy loss of bearing, high-speed rotation, rotor vibration and noise. The vibration control of the flywheel with active magnetic bearing is being studied for gyroscopic stability of artificial satellite[4],[5].

There are different control types of AMB, the axial direction (one degree of freedom; 1DOF)control, the radial direction(2 or 4 DOF) control and the omni-directional(5 DOF) control[6]. The omni-directional control type of AMB, which is analyzed in this paper, can control the motion of the center of gravity (3 DOF)and the declination around the center of gravity(2 DOF). The control system has to take into account the dynamics of rotor-disk coupled system, that is, the low frequency backward instability and high frequency forward instability due to strong gyroscopic effect. The study of the stability using cross stiffness control has been reported[4],[7].

In this paper, an equivalent reduced model of the rotor is completed from the quasi-modal method. The obtained model is applied to design and evaluation of the rotor dynamics combined with the servo feedback control theory of the AMB system.

The PID control theory is popular in practical engineering and we employed it for the levitation control. Due to the gyroscopic effect at high-speed rotation, the natural frequencies are split into two ways: the backward motion is low and forward motion is high. The prepared PID controller is then not able to cover the stability in the entire speed range. In order to compensate this insufficiency of the PID controller, the introduction of the cross stiffness control is successfully demonstrated with the combination of a band-pass filter for tuning the high frequency vibration of the forward mode and a low-pass filter for low frequency backward mode.

We also take into account the rotor-disk coupled dynamics due to disk bending flexibility which made the system stabilization difficult. According to the simulations, our PID control method combined with optional techniques made the stabilization control and the reduction of unbalance vibration level for global conditions of standstill and rotation.

2 MODEL

2.1 Flywheel

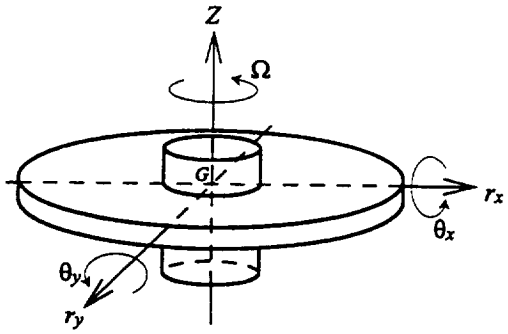

Fig.1 Rotor coordinate system

Fig.1 shows the structure of the flywheel model and the coordinate system. The equation of motion of the flywheel and AMB neglecting the damping term can be expressed as follows[6]:

$$\text{Axial}: M\ddot{Z} + K_a Z = -Q_{AMBa} \quad (1a)$$

$$\text{Tilting}: I_d\ddot{\theta} - i\Omega I_p\dot{\theta} + K_\theta\theta = -lQ_{AMBa} \quad (1b)$$

$$\text{Radial}: Mr + Kr = -Q_{AMBr} \quad (1c)$$

Where:

Z : the displacement in the axial direction
M : the rotor mass matrix
K_a : the stiffness matrix in the axial direction
Q_{AMBa} : the axial AMB control force matrix
I_d : the tilting inertia moment
θ : the complex declination angle($\theta x + i\theta y$)
I_p : the inertia moment of flywheel
K_θ : the tilting stiffness matrix
l : the length from geometrical center of the flywheel to geometrical center of axial AMB
r : the complex displacement($rx + iry$)
K : the stiffness matrix
Q_{AMBr} : the radial AMB control force

The modeling is analyzed by quasi-modal model based on the component mode synthesis[8]. The flywheel consists of a motor-rotor and an elastic disk. The coupled vibration of the rotor-disk is shown in Table1[9]. We can see there are only two coupled vibration in Table 1(see the O). Therefore the model is included eigenmodes of the disk, the coupled axial mode of the rigid motor-rotor δ_a with one nodal circle mode ϕ_a and the coupled tilting mode of the rigid motor-rotor δ_t with one nodal diameter mode ϕ_t [10]. These modes in the axial direction and the tilting direction are shown in Fig.2. The axial and the tilting motion are considered as independent.

Table 1 Coupled Vibration of Rotor-disk System

Disk Modes (Flexible)	Nodal-Diameter	0	....	1	2	....
	Nodal-Circule	1	....	0	0	....
Rortor Modes (Rigid)	Axial Z	O	×	×	×	×
	Tilting θ	×	×	O	×	×
	Radial r	×	×	×	×	×

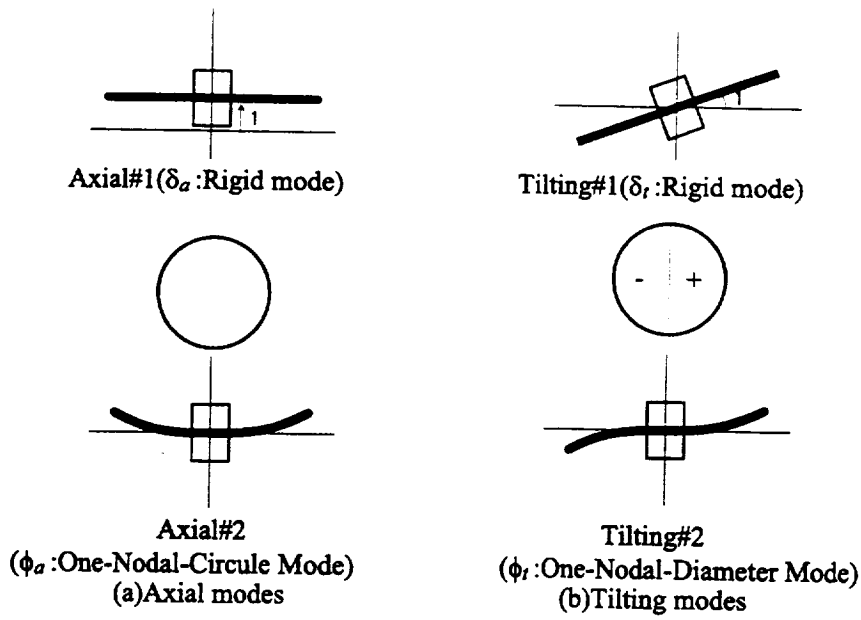

Fig.2 Flywheel Rotor Displacement Modes

The displacement vector, absolute displacement of the rotor; Z_1, θ_1, and internal displacement of the disk; Z_2, θ_2, can be expressed in terms of the rotor Z_1 , θ_1 and the relative displacement of disk η_a, η_t by the following formula:

$$Z=\begin{bmatrix}Z_1\\Z_2\end{bmatrix}=\begin{bmatrix}1 & 0\\ \delta_a & \phi_a\end{bmatrix}\begin{bmatrix}Z_1\\ \eta_a\end{bmatrix}=\Phi_a\begin{bmatrix}Z_1\\ \eta_a\end{bmatrix} \quad (2a), \qquad \theta=\begin{bmatrix}\theta_1\\ \theta_2\end{bmatrix}=\begin{bmatrix}1 & 0\\ \delta_t & \phi_t\end{bmatrix}\begin{bmatrix}\theta_1\\ \eta_t\end{bmatrix}=\Phi_t\begin{bmatrix}\theta_1\\ \eta_t\end{bmatrix} \quad (2b)$$

where, Φ_a, Φ_t are the component mode synthetic conversion matrix. Substituting Eq.(1a) and Eq.(1b) for Eq. (2a) and Eq.(2b), and the transposed matrix of Φ_a, Φ_t multiplied from the front in order to make the quadratic form, the equation of motion of the rotor can be obtained as in Eq.(3a) and (3b) .

$$\text{Axial}: \begin{bmatrix}m & m_{ca}\\ m_{ca} & m_D^{\bullet}\end{bmatrix}\begin{bmatrix}\ddot{Z}_1\\ \ddot{\eta}_a\end{bmatrix}+\begin{bmatrix}k_a & \\ & k_{aD}\end{bmatrix}\begin{bmatrix}Z_1\\ \eta_a\end{bmatrix}=-\begin{bmatrix}Q_{AMBa}\\ 0\end{bmatrix} \quad (3a)$$

$$\text{Tilting}: \begin{bmatrix}I_d & i_{dc}\\ i_{dc} & i_{dD}^{\bullet}\end{bmatrix}\begin{bmatrix}\ddot{\theta}_1\\ \ddot{\eta}_t\end{bmatrix}-i\Omega\begin{bmatrix}I_p & i_{pc}\\ i_{pc} & i_{pD}^{\bullet}\end{bmatrix}\begin{bmatrix}\dot{\theta}_1\\ \dot{\eta}_t\end{bmatrix}+\begin{bmatrix}k_\theta & \\ & k_{\theta D}\end{bmatrix}\begin{bmatrix}\theta_1\\ \eta_t\end{bmatrix}=-\begin{bmatrix}lQ_{AMBa}\\ 0\end{bmatrix} \quad (3b)$$

m: total mass

$m_D^{\bullet}=m_D\phi_a^2$: modal mass of disk, $i_{dD}^{\bullet}=i_{dD}\phi_t^2$: modal tilting inertia moment of disk

m_D: mass of disk, i_{dD} : tilting inertia moment of disk

m_{ca} : mass compound terms, i_{dc}, i_{pc}: inertia compound terms

Eq.(3a) and (3b) represents the disk bending modes by the relative displacement. The absolute displacement of the bending modes are indicated by ξ_a and ξ_t. It is assumed with ξ_a-Z_1 and ξ_t-θ_1 in proportion to η_a and η_t. We define the quasi-modal matrix T.

$$\begin{bmatrix} Z_1 \\ \eta_a \end{bmatrix} = T\begin{bmatrix} Z_1 \\ \xi_a \end{bmatrix} = \begin{bmatrix} 1 & 0 \\ -a_a & a_a \end{bmatrix}\begin{bmatrix} Z_1 \\ \xi_a \end{bmatrix} \qquad (4a)$$

$$\begin{bmatrix} \theta_1 \\ \eta_t \end{bmatrix} = T\begin{bmatrix} \theta_1 \\ \xi_t \end{bmatrix} = \begin{bmatrix} 1 & 0 \\ -a_t & a_t \end{bmatrix}\begin{bmatrix} \theta_1 \\ \xi_t \end{bmatrix} \qquad (4b)$$

where a_a and a_t are determined to cancel the mass compound terms in Eq(3a),(3b).

$$a_a = {m_{ca}}/{m_D^*} = {m_D\phi_a}/{m_D\phi_a^2} \qquad (5a)$$

$$a_t = {i_{dc}}/{i_{dD}^*} = {i_{dD}\phi_t}/{i_{dD}\phi_t^2} \qquad (5b)$$

Finally, the equation of motion of the quasi-modal model is as Eq.6 and the quasi-modal model is shown Fig.3.

$$\begin{bmatrix} m_m + \Delta m_D & \\ & m_{Deq} \end{bmatrix}\begin{bmatrix} \ddot{Z}_1 \\ \ddot{\xi}_a \end{bmatrix} + \begin{bmatrix} k_a + k_{Deq} & -k_{Deq} \\ -k_{Deq} & k_{Deq} \end{bmatrix}\begin{bmatrix} Z_1 \\ \xi_a \end{bmatrix} = -\begin{bmatrix} Q_{AMBa} \\ 0 \end{bmatrix} \qquad (6a)$$

$$\begin{bmatrix} I_{dm} + \Delta i_{dD} & \\ & i_{dDeq} \end{bmatrix}\begin{bmatrix} \ddot{\theta}_1 \\ \ddot{\xi}_t \end{bmatrix} - i\Omega\begin{bmatrix} I_{pm} + \Delta i_{pD} & \\ & i_{pDeq} \end{bmatrix}\begin{bmatrix} \dot{\theta}_1 \\ \dot{\xi}_t \end{bmatrix} + \begin{bmatrix} k_\theta - k_{D\theta eq} & -k_{D\theta eq} \\ -k_{D\theta eq} & k_{D\theta eq} \end{bmatrix}\begin{bmatrix} \theta_1 \\ \xi_t \end{bmatrix} = -\begin{bmatrix} lQ_{AMBa} \\ 0 \end{bmatrix} \qquad (6b)$$

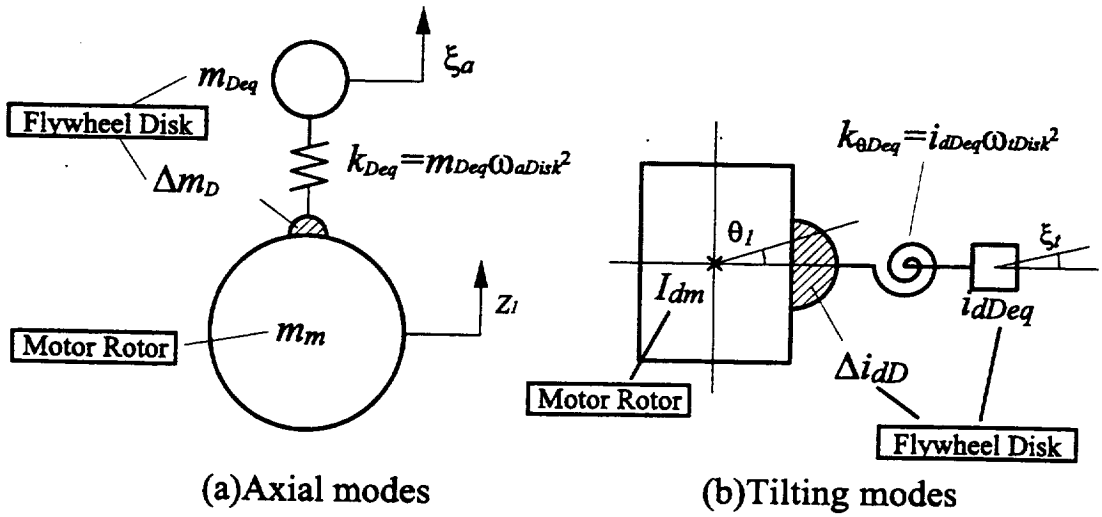

Fig.3 Quasi-modal Models
(Equivalent Reduction System)

2.2 Flywheel Test Rotor System

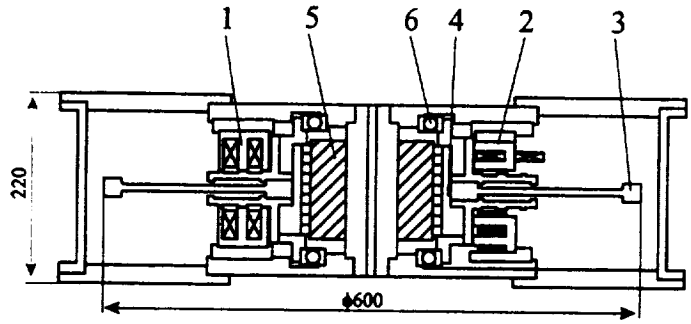

1:Axial AMB 2:Radial AMB 3:Flywheel Disk
4:Motor-Rotor 5:Motor-Stator 6:Auxiliary Bearing

Fig.4 Schematic of Flywheel

Schematic of flywheel test rotor is shown in Fig.4. The main characteristics of the flywheel is as follows:

Flywheel Diameter : 0.6m
Rotor mass : 36kg
Inertia moment : 0.69kgm^2
Max. rotational speed : 200rps

2.3 Active Magnetic Bearing(AMB)

The coordinate system and outline of the magnetic bearings are shown in Fig.5 and 6, respectively. The axial AMB has three displacement sensors arranged at each actuator and feeds back the sensing data directly. Displacement output Z_a, Z_b, Z_c measured by each sensor is changed into declination θ and displacement Z_1 of the axis center of gravity by conversion matrix $T_{z\theta}$ shown in Eq.(7).

$$\begin{bmatrix} Z_a \\ Z_b \\ Z_c \end{bmatrix} = T_{Z\theta} \begin{bmatrix} Z_1 \\ \theta_x \\ \theta_y \end{bmatrix} = \begin{bmatrix} 1 & -l & 0 \\ 1 & l\sin 30^\circ & l\sin 30^\circ \\ 1 & l\sin 60^\circ & -l\sin 60^\circ \end{bmatrix} \begin{bmatrix} Z_1 \\ \theta_x \\ \theta_y \end{bmatrix} \tag{7}$$

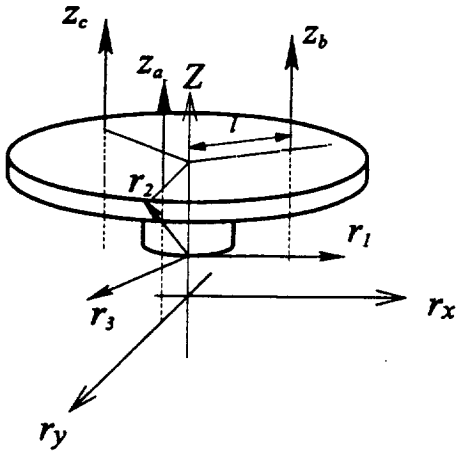

Fig.5 Coordinate Frame of AMB

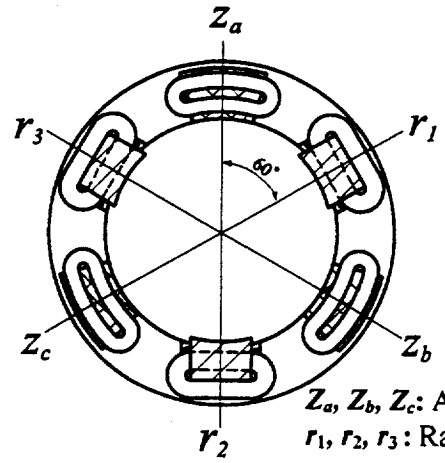

Z_a, Z_b, Z_c: Axial AMB
r_1, r_2, r_3: Radial AMB

Fig.6 AMB Actuator Assembly

Radial displacement sensors have been installed in the 2 directions of r_x and r_y (Fig. 7). The three directional deviations, which is used to control radial direction, are computed from two deviations between the AMB reference inputs and exact gaps using the conversion matrix T_r, shown in Eq. (8).

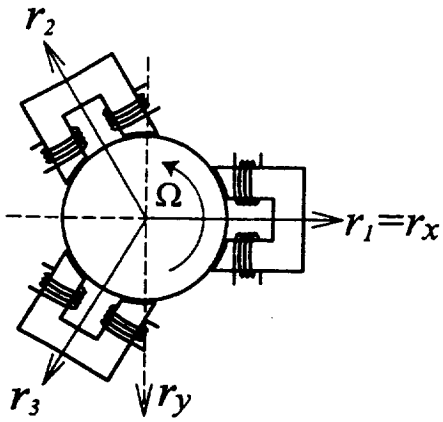

$$\begin{bmatrix} r_1 \\ r_2 \\ r_3 \end{bmatrix} = T_r \begin{bmatrix} r_x \\ r_y \end{bmatrix} = \begin{bmatrix} 1 & 0 \\ -\cos 60^\circ & -\cos 30^\circ \\ -\cos 60^\circ & \cos 30^\circ \end{bmatrix} \begin{bmatrix} r_x \\ r_y \end{bmatrix} \quad (8)$$

Fig.7 Active Magnetic Bearing Actuator (6pole Type Radial AMB)

Using this conversion, it is possible to control three actuators independently. The whole composition of AMB is shown in Fig. 8 and the main specification is shown in table 2.

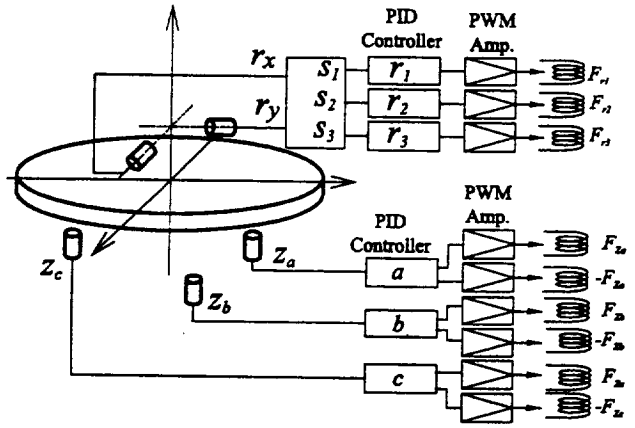

Fig.8 Block Diagram of The Electronics System

Table 2 Main Parameter of AMB

	Axial AMB	Radial AMB
Load Capacity	557 N	332 N
AMB Clearance	0.3×10^{-3}m	0.5×10^{-3}m
Sensor Gain	10000 V/m	10000 V/m
Power Amp. Gain	2 A/V	2 A/V

3 EIGENVALUE ANALYSIS

3.1 Critical Map

The critical map of this rotor system is shown in Fig. 9. The horizontal axis is the stiffness of AMB and the vertical axis is the natural frequency. Each line indicates the natural frequency of the first rigid mode (Axial), the second rigid mode (Tilting), the first bending mode (Axial) and the second bending mode

(tilting) from downward to upward, respectively. When the stiffness of AMB is set to $3x10^5$ N/m, the natural frequency of the rigid mode (Axial) is fixed about 30 Hz. The resonance oscillated by a disturbance, e.g., earthquakes, is prevented using this tuning (setting the natural frequency to less than 10 Hz).

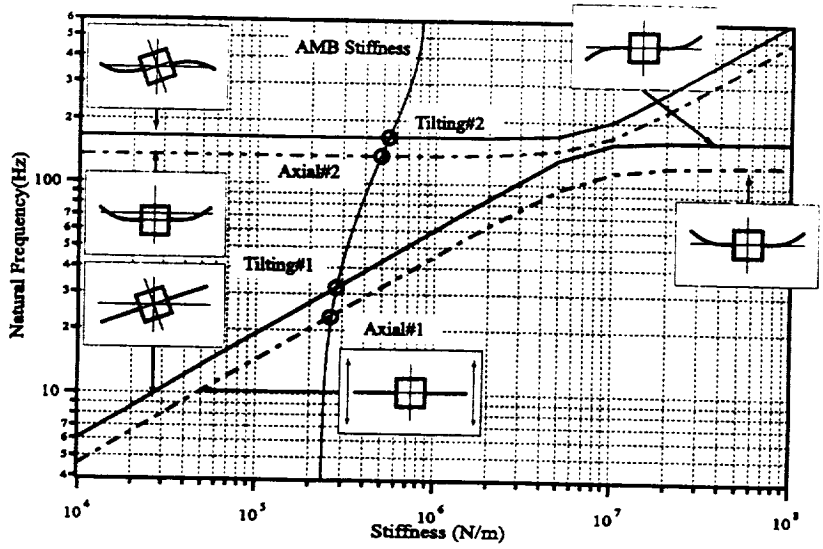

Fig.9 Critical map with AMB Stiffness (Standstill)

3.2 Eigenvalue Map

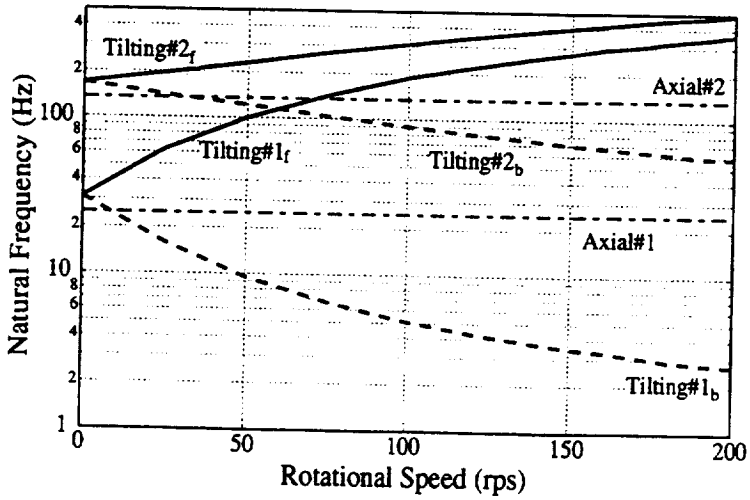

Fig.10 Eigenvalue Map

The eigenvalue map (Campbell diagram) is shown in Fig. 10. The horizontal axis is the rotational speed of flywheel and the vertical axis is a frequency. The solid lines indicate the natural frequency of the first and the second forward tilting (Tilting#1 and #2) mode, the dashed lines indicate the natural frequency the first and the second backward tilting (Tilting#1b and #2b) mode and the dot-dashed lines indicate the natural frequency of axial (Axial#1 and #2) mode. The axial natural frequencies are constant (the rigid mode is 23 Hz and the bending mode is 137 Hz) because no gyroscopic force is affected to the axial direction. However, the tilting natural frequency changes with the rotational speed due to the effect of gyroscopic force. The natural frequency of the forward motion is more than 400 Hz at 200 rps and the natural frequency of the backward motion is less than 10 Hz.

4 DESIGN OF CONTROL SYSTEM

4.1 Control System

The control system of the experimental device is shown in Fig.11. The AMB levitates the flywheel with the feedback control using the signal from the displacement sensor without the mechanical contact. The control system executes analog PID control in the axial and radial directions. The phase progress is up to 200 rps in the transfer function, allowing damping addition against the unbalance vibration. The phase progress is from 10Hz to 400Hz by the characteristics of the PID controller and PWM amplifier. The bode diagram is shown in Fig.12.

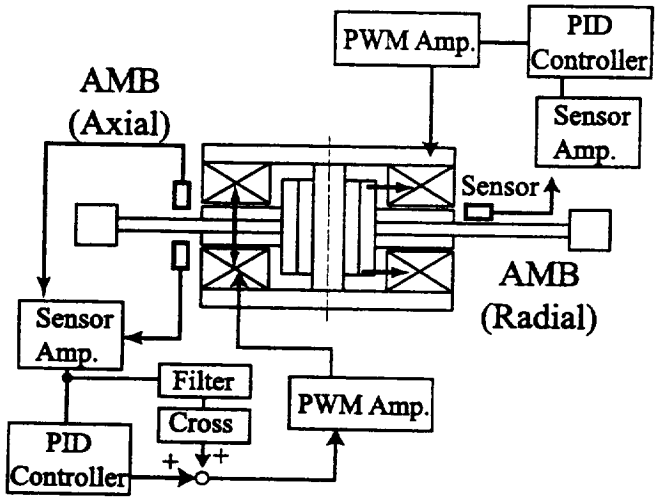

Fig.11 Block Diagram of AMB Control System (with Cross Stiffness)

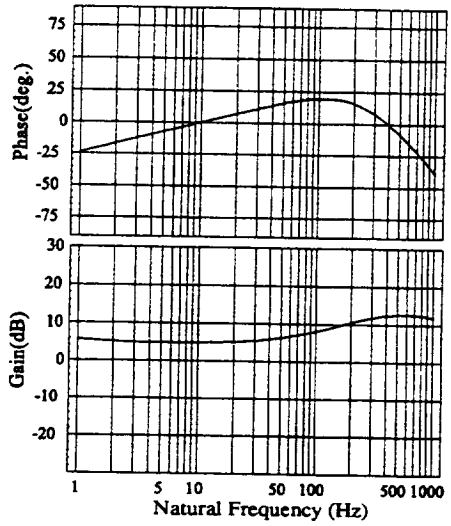

Fig.12 Basic Control Low (PID Controller)

4.2 Stability Analysis and Design of Controller

We simulate the flywheel rotation test including the controller in the axial, tilting and radial direction. It is expected not to be stable with only PID control. The controller is added against the forward motion and the backward motion due to tilting gyroscopic effect.

4.2.1 Control in the tilting direction

The tilting natural frequency changes by gyroscopic effect. The natural frequency of the forward motion is more than 400Hz with 200 rps rotation speed and the frequency of the backward is less than 10Hz. The PID controller does not have the damping in more than 400 Hz because of the phase lag. It is unstable below 10 Hz because of integral compensation which removes the steady error. The stability using cross stiffness control is useful for these cases[4],[7]. However, the cross stiffness to stabilize one makes the other unstable.

We use two types of displacement cross stiffness control in the unstable area. In order to compensate this insufficiency of PID controller, we recommend the addition of optional techniques such as, Band-Pass-Filter(BPF) and Low-Pass-Filter(LPF) cross stiffness control for tilting mode. The BPF cross stiffness control for more than 150rps rotational speed completes the stabilization against the forward motion. The transfer function is as follows:

$$G_{BPFCross}(s) = G_{BPF}(s) \cdot (-ik_c), \quad G_{BPF}(s): \text{The Transfer Function of BPF} \tag{9}$$

The LPF cross stiffness control completes the stabilization against the backward motion. The transfer function is as follows:

$$G_{LPFCross}(s) = \frac{ik_c}{\tau s + 1}, \quad \tau = \frac{1}{2\pi \times 6} \tag{10}$$

Therefore, the controller gives the stability against the forward and backward motion due to tilting gyroscopic effect.

4.2.2 Control in the radial direction

The natural frequency is about 30Hz in the radial direction. There is no gyroscopic effect. Therefore the stability is given by the PID controller only. Because there is only the rigid mode within the operational speed, addition of N-Cut control[11] is able to prevent the instability caused by unbalance vibration after passing of the rigid mode.

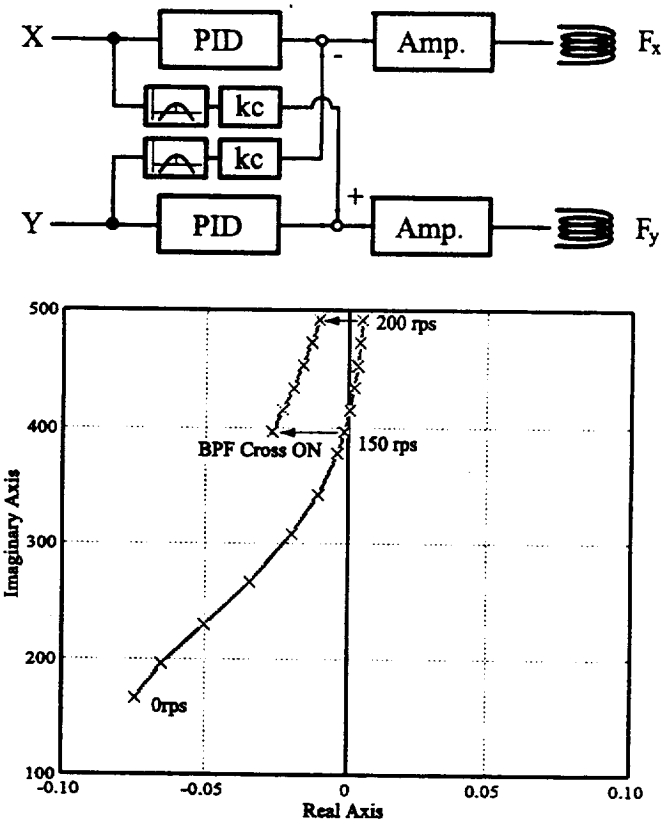

Fig.13 Root Locus with BPF Cross Stiffness (Tilting#2 Forward Whirl)

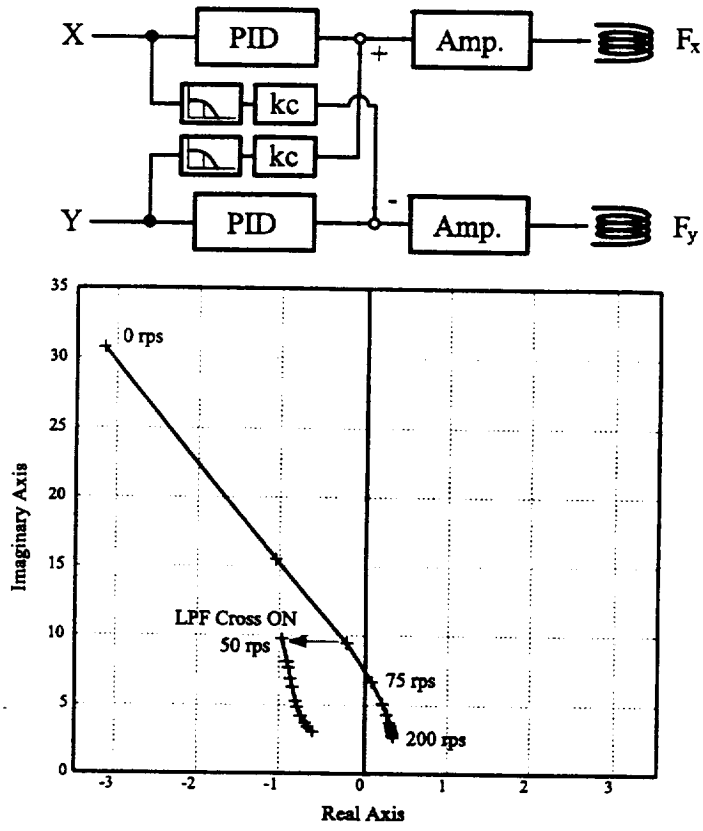

Fig.14 Root Locus with LPF Cross Stiffness (Tilting#2 Backward Whirl)

5 CONCLUSION

We discussed the stability improvement by the AMB control system including the design review of our flywheel test rotor.

(1) Our AMB equipped flywheel is featured by a 5DOF control of three axes for the vertical suspension control and two axes for radial positioning control.
(2) A reduced model is obtained by quasi-modal modeling, which considers the gyroscopic effect and disk bending flexibility.
(3) The instability induced by the strong gyroscopic effect for flat disk and the compensation by the cross stiffness control is evaluated. The cross stiffness in combination with the filter to select only unstable vibrations is strongly recommended by the simulation.
(4) The spill over instability due to the disk flexibility is eliminated by preparing wide control frequency domain covering the disk bending eigenfrequencies..
(5) The design review of our flywheel test rotor is achieved.

REFERENCES

(1) Stienmier, J. D. et al., Analysis and control of a flywheel energy storage system with a hybrid magnetic bearing, Trans. ASME, J. Dyn. Syst. Meas. Control, vol.119, no.4(1997), p.650

(2) Higasa, H. et al., Technical Problems of Superconducting Magnetic Bearing and Construction of Flywheel Power Storage System, *Proc. of ISS'93(1993)* p.1231

(3) Jayaraman, C. P. et al., Rotor dynamics of flywheel energy storage systems, Trans. ASME, J. Sol. Energy Eng., vol.113, no.1(1991), p.11

(4) Inoue, M., High-speed test and the gyroscopic stability of the magnetically suspended wheel, Trans. Soc. Instrum. & control Eng. (In Japanese), vol.23, no.3(1987), p.294

(5) Ohshima, T. et al., Stabilization of satellite equipped with a magnetically suspended momentum wheel, Trans. Soc. Instrum. & control Eng. (In Japanese), vol.27, no.2(1991), p.192

(6) Higuti, T. et al., Control system design for totally active DC-type Magnetic bearing, Trans. Soc. Instrum. & control Eng. (In Japanese), vol.18, no.5(1982), p.79

(7) Matsushita, O. et al., Cross stiffness control of electromagnetic damper for flow-induced rotor instability, *Proc. of Elastic Aero Hydrou Engineering'99(1999)*

(8) Matsushita, O., Modering; Free from boundary condition, Jpn. Soc. Prec. Eng. (In Japanese), vol.54, no.5(1988),p.44

(9) Irretier, H. et al., Numerical and experimental investigations of coupling effects in an isotropic elastic rotors, *Proc. of IFToMM Conf. on Rotor Dynamics 1998*, p.296

(10) Matsushita, O. et al., An equivalent reduced system for coupled vibration analysis, Trans. Jpn. Soc. Mech. Eng., vol.54, no.499,C, p.587

(11) Matsushita, O. et al., Optional techniques for active magnetic bearing equipped flexible rotors, *Proc. of IFToMM Conf. on Rotor Dynamics 1998*